*Proceedings of the 21st International Conference on Global Research and Education (Inter-Academia 2024)*

# Protective Implant for the Femoral Neck in Osteoporosis Patients

M. Urban[a,*], I. Stencel[b], J. Dziedzic[b] and S. Cygan[a]

[a]*Faculty of Mechatronics, Institute of Metrology and Biomedical Engineering, Warsaw University of Technology, św. A. Boboli 8, 02-525 Warsaw, Poland*
[b]*Faculty of Mechatronics, Institute of Micromechanics and Photonics, Warsaw University of Technology, św. A. Boboli 8, 02-525 Warsaw, Poland*

Doi: 10.12693/APhysPolA.146.585 *e-mail: mateusz.urban2.stud@pw.edu.pl

This study proposes a new type of femoral neck reinforcement implant for patients suffering from osteoporosis. The aim of the implant is to prevent fractures of this part of the bone. Implant designs in six variants have been simulation-tested in two situations: a typical static load and a simulated dynamic load, in which the force was applied in a manner corresponding to a sideways fall. The tests were carried out for six different biocompatible materials, i.e., three polymeric and three titanium alloys from which the implants could be made. The obtained results tentatively demonstrated the validity of the proposed concept and allowed the design with the best properties to emerge. In addition, they showed that the use of a polymeric material, in particular polylactide, leads to a more substantial reduction in maximum stress values.

topics: osteoporosis, bone fracture, finite element analysis

## 1. Introduction

Osteoporosis is a condition characterised by reduced average bone density, bone tissue degradation, and changes in the micro-architecture of bones. These changes result in a decrease in bone strength and an increased risk of fracture even at low loading [1, 2].

The causes of osteoporosis, also known as the "silent disease" due to the lack of visible symptoms of the development of the condition until a fracture occurs, are usually, but not always, age-related. One of the most common causes is the occurrence of a permanent break in sex hormone production, i.e., a lack of oestrogen production in women (menopause) or a corresponding lack of testosterone production in men (andropause) [3]. Other common causes of osteoporosis may be vitamin D deficiency and high salt intake, which may be correlated with the place of residence and the typical lifestyle of the region (Fig. 1) [4]. Studies carried out in various countries indicate that it is the Scandinavian people who rank as the ones most at risk of developing osteoporosis among the entire group studied [5].

Other causes of osteoporosis include genetic, gastrointestinal, rheumatological, and autoimmune diseases, haematological disorders and neurological and musculoskeletal factors [3].

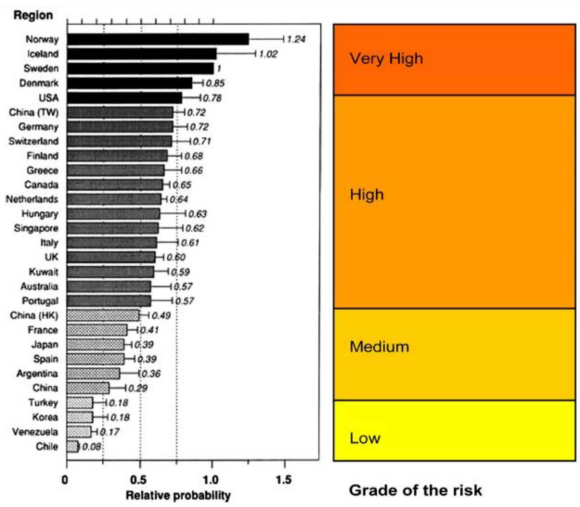


Fig. 1. Probability of hip fractures averaged for age and sex over a ten-year period for a given region with reference to Sweden for 2002 [4].

In 2019, an estimated 22.1% of women and 6.6% of men in the European Union over the age of 50 could be affected by osteoporosis, which is approximately 32 million people [6]. Worldwide, in the same year, there were almost 37 million osteoporosis-related fragility fractures in people over 55, of which

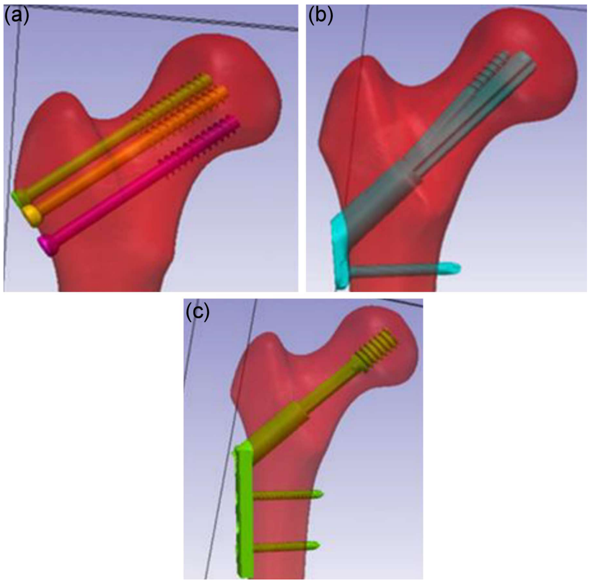


Fig. 2. Three methods of femoral neck stabilisation used in a study conducted at the Yale University [16].

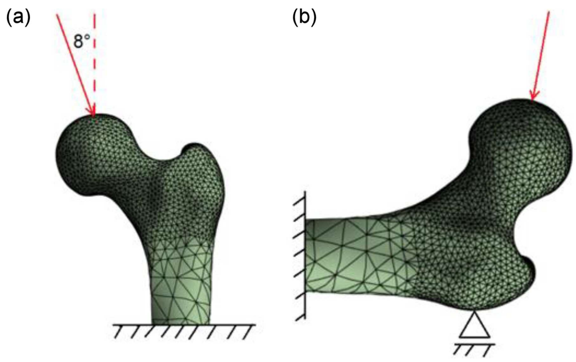


Fig. 3. Boundary conditions used in the simulation: (a) statically loaded bone model, (b) dynamically loaded bone model [19].

more than 10 million were hip fractures [7]. The mortality rate of hip fracture in patients with osteoporosis is approximately 20% within a year of fracture, mainly through pre-existing medical conditions [8, 9]. On the other hand, 40% of patients are unable to continue to move independently, and 33% are totally dependent or placed in seniors' homes [9]. Other consequences of such a fracture can be chronic pain, reduced mobility, and total or increasing disability over time [8, 10].

Currently, the most common method for a femoral neck fracture is to remove the entire proximal end of the femur and insert an endoprosthesis to act as a hip joint [11, 12]. However, this procedure is quite risky, and the patient often has to stay in bed for several months after the procedure to make sure that the implant has taken, which in the case of older people can have a negative impact on

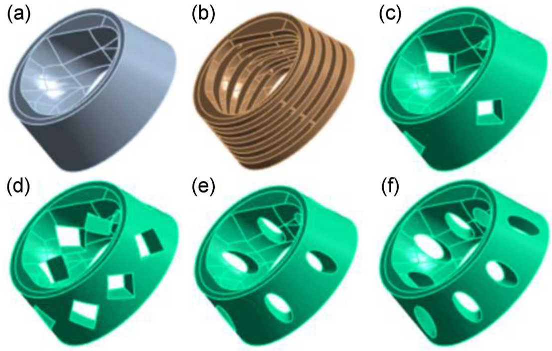


Fig. 4. The implant shapes used in the simulation: (a) "pure" — a solid, bone-matched ring, (b) "pins" — a ring composed of plates connected by pins, (c) "square 4" — a ring with 4 evenly spaced quadrilateral holes, (d) "square 8" — ring with 8 evenly spaced quadrilateral holes, (e) "ellipse 6" — ring with 6 evenly spaced elliptical holes, (f) "ellipse 8" — ring with 8 evenly spaced elliptical holes.

their further life expectancy [13]. Sometimes, such an implant, after prolonged use, may loosen spontaneously as a result of fatigue changes and material ageing. In this case, the procedure must be repeated, with the removal of another fragment, this time of already dead bone [14, 15].

A Yale University research team investigating an implant designed to protect the femoral neck from fracture (Fig. 2) [16] has developed an alternative to removing part of the bone and inserting an implant to replace the entire hip joint. Screw and flat bar systems were used to reinforce the region of the femur under study. Unfortunately, the proposed solutions violate the red marrow located in the epiphysis of the long bones, which is responsible for haematopoietic processes [17].

The aim of the present study was to design and numerically test an implant with a similar function that would be placed on the bone surface to reduce the risk of red bone marrow damage.

## 2. Materials and methods

### 2.1. Bone model

Developing the model for simulation involved collecting and configuring all the necessary data in Ansys software, i.e., creating a list of implant materials and shapes, acquiring and importing the bone model, and establishing the boundary conditions (fixings and loads) and mechanical properties of the material.

Since the male and female skeletal systems differ in structure, it was decided to obtain a model of the female femur, since, as mentioned earlier, women are more than 3 times more likely to develop

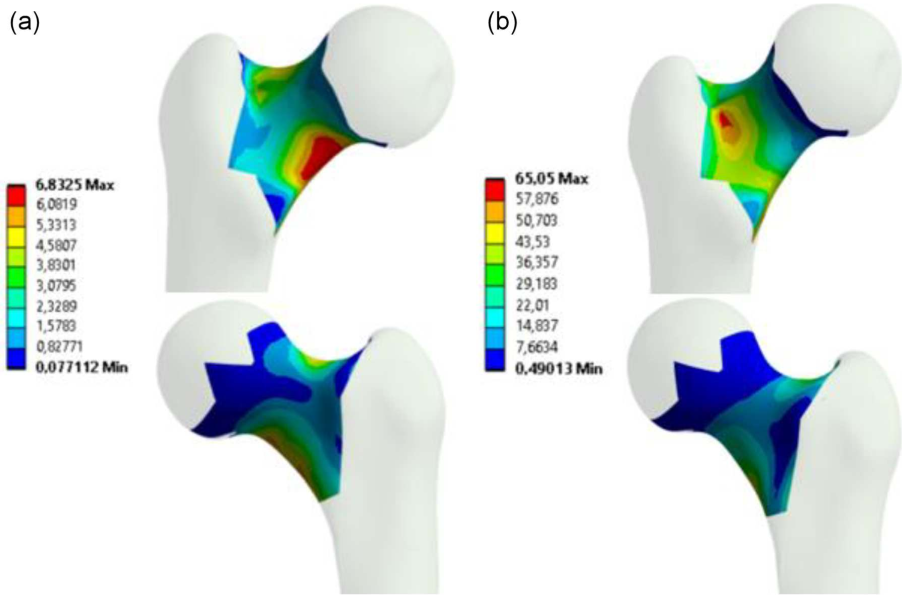


Fig. 5. Stress maps for both loading variants of the diseased bone without additional implants: (a) static, (b) dynamic.

TABLE I

List of biocompatible materials used in the simulation.

| Name | Abbrev. | Poisson's ratio | Young's modulus [GPa] | Density [g/cm$^3$] |
|---|---|---|---|---|
| Polylactide | PLA | 0.36 | 1.90 | 1.25 |
| Polisulfone | PSU | 0.37 | 2.65 | 1.24 |
| Poly(methyl methacrylate) | PMMA | 0.35 | 2.55 | 1.18 |
| Ti–12Mo–6Zr–2Fe | Ti-12 | 0.33 | 82.5 | 4.82 |
| Ti–35Nb–5Ta–7Zr | Ti-35 | 0.35 | 57.5 | 5.51 |
| Ti–13Nb–13Zr | Ti-13 | 0.34 | 77.5 | 5.04 |

osteoporosis. The model was obtained from the US National Institutes of Health website [18] and implemented for simulation in Ansys.

In the *finite element analysis* (FEA) simulation, it was necessary to assign appropriate mechanical properties to the bone since the aim of the project was to develop an implant that would reduce the stresses arising in osteoporotic bone, which could result in fracture. A set of mechanical parameters was prepared for such a bone, on which all simulations were carried out [19, 20].

In order to perform the simulation correctly, it was also necessary to establish the boundary conditions of the simulation, i.e., how the bone was fixed and what forces acted on it (Fig. 3) [19]. Two cases had to be considered: (i) static, i.e., loads occurring during standing or walking [16, 19], and (ii) dynamic, i.e., loads occurring during a fall [19, 21].

A number of implant designs were prepared for the study, with the inner surface reproducing the shape of the reinforced femoral neck (Fig. 4). A list of materials whose mechanical parameters were used for the study is presented in Table I.

## 2.2. Simulation

Simulation studies carried out in the Ansys environment included stress modelling of bone without an implant and with all proposed implants made of all materials (Table I). This gave a total of 72 possible design–material combinations to test.

## 3. Results

As a first step, a control simulation was carried out for both cases considered (static and dynamic loading) in order to obtain the maximum stresses occurring and how they are distributed in the bone region under study (Fig. 5). The results obtained were 6.83 MPa for the static conditions and 65.05 MPa for the dynamic conditions.

Next, 36 variants of shape–material pairs were simulated for static loading. The results are shown in Table II. The results of the series of simulations carried out for the assumed dynamic loads are shown in Table III.

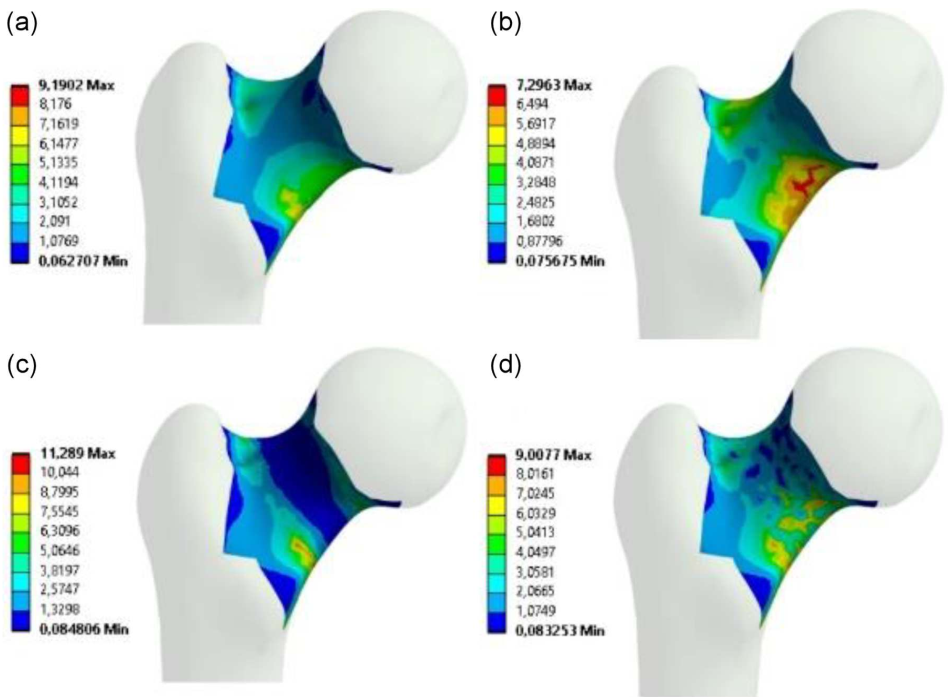


Fig. 6. Stress distributions under static loading for implants with different geometries and materials: (a) "pure" made of PLA, (b) "pins" made of PLA, (c) "pure" made of Ti-35, (d) "pins" made of Ti-35.

TABLE II

Maximum stresses for the affected bone, in the static case, depending on the geometry and material used, given in MPa.

| Material | Pure | Pins | Square 4 | Square 8 | Ellipse 6 | Ellipse 8 |
|---|---|---|---|---|---|---|
| PLA | 9.19 | 7.3 | 9.12 | 9.61 | 9.23 | 6.78 |
| PSU | 9.55 | 7.38 | 9.48 | 9.91 | 9.62 | 9.24 |
| PMMA | 9.49 | 7.37 | 9.43 | 9.86 | 9.56 | 9.2 |
| Ti-12 | 11.5 | 9.56 | 11.9 | 11.7 | 11.54 | 11.71 |
| Ti-35 | 11.3 | 9.01 | 11.8 | 11.6 | 11.45 | 11.52 |
| Ti-13 | 11.5 | 9.47 | 11.9 | 11.7 | 11.51 | 11.68 |

TABLE III

Maximum stress for the affected bone, in the dynamic case, depending on the geometry and material used, given in MPa.

| Material | Pure | Pins | Square 4 | Square 8 | Ellipse 6 | Ellipse 8 |
|---|---|---|---|---|---|---|
| PLA | 75.8 | 64.7 | 74.8 | 76.1 | 75.4 | 64.5 |
| PSU | 79.4 | 64.6 | 78.3 | 78.8 | 78.9 | 76.5 |
| PMMA | 78.9 | 64.6 | 77.8 | 78.4 | 78.4 | 76.1 |
| Ti-12 | 109.8 | 72.1 | 109.2 | 106.4 | 107.2 | 105.4 |
| Ti-35 | 107.7 | 70.5 | 106.4 | 104.2 | 105.2 | 103 |
| Ti-13 | 109.4 | 71.8 | 108.8 | 106. | 106.8 | 105 |

Figures 6 and 7 show the stress distribution maps for the static and dynamic loading cases for the "pure" implant and the "pin" model, respectively, for the polymer material and the titanium alloy that produced the lowest stresses.

## 4. Conclusions

The first thing that can be observed is the changes in stress distribution that occur under different types of loading without and with an implant. In both load variants, the stress distribution with polymer implants did not change much, but single points were created that can cause fractures. With titanium alloy implants, there was stress relief in the mid-neck region and stress accumulation at the extremities of the implant.

When stress values are considered, it can be seen that the lowest values were obtained with the "pins" shaped implant. However, the lowest stresses for both cases were obtained for the "ellipse 8" made of *polylactide* (PLA). This result does not fit into the trends of the other results, suggesting the need to approach this result critically.

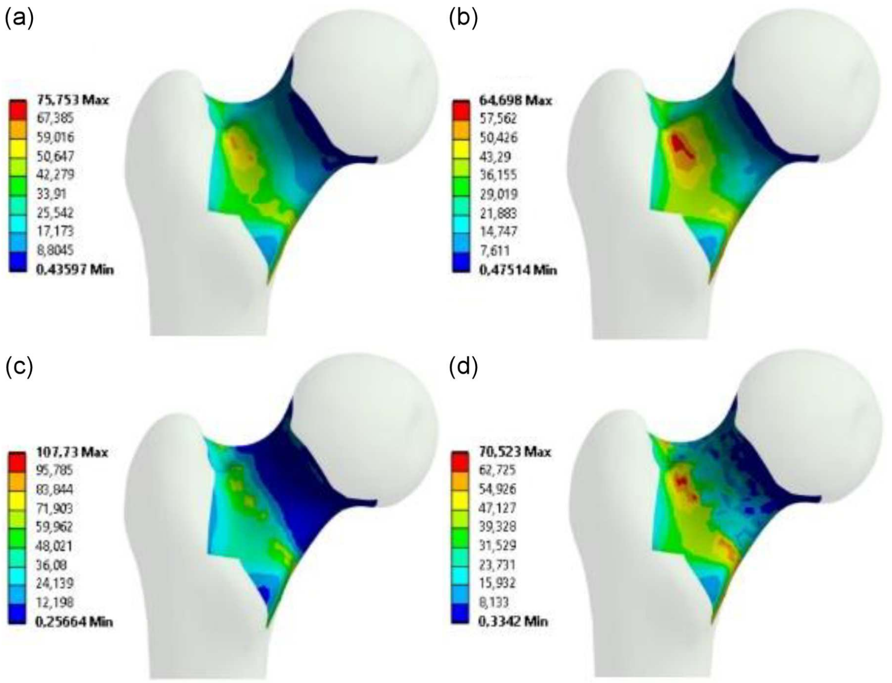


Fig. 7. Stress distributions under dynamic loading for implants with different geometries and materials: (a) "pure" made of PLA, (b) "pins" made of PLA, (c) "pure" made of Ti-35, (d) "pins" made of Ti-35.

When considering implants by material, it can be seen that, within the polymer group, the lowest stresses were in bone with a polylactide implant. Unfortunately, this material is biodegradable and becomes brittle at high stresses, which would carry a risk for the patient. In the case of the titanium alloy group, Ti-35 behaved best. As this is one of the materials commonly used for hip endoprostheses, it can also be assumed that it would work well as an implant material to support still-living tissue.

From the results obtained, the best combination with development potential would be an implant with a ribbed design resembling a "pins"-type, spanning the neck from the head to the greater vertebral body to transfer loads from the neck to the stronger areas. A composite with a polymer-matrix titanium alloy core could be used as the material to provide a "cushion" to absorb the stresses transmitted by the implant.

The results of this study are preliminary. In future work, instead of a simplified bone model, a simulation with the exact density distribution of the individual bone tissues can be designed. The simulation can additionally consider the increase in anisotropy of the bone tissue progressing with age in order to obtain results as close to reality as possible. Once the optimum implant shape and material have been obtained, fabrication technology and placement in the patient's body could be considered. The next step could be testing bone preparations as a means of validating and verifying the simulation results.

## References

[1] T. Sözen, L. Özışık, NÇ. Başaran, *Eur. J. Rheumatol.* **4**, 46 (2017).

[2] A. Sheik Ali, *Cureus* **15**, e43031 (2023).

[3] F. Pouresmaeili, B. Kamalidehghan, M. Kamarehei, Y.M. Goh, *Ther. Clin. Risk Manag.* **14**, 2029 (2018).

[4] L. Sŕnchez-Riera, N. Wilson, N. Kamalaraj et al., *Best Pract. Res. Clin. Rheumatol.* **24**, 793 (2010).

[5] D. Felsenberg, A.J. Silman, M. Lunt et al., *J. Bone Miner. Res.* **17**, 716 (2002).

[6] J.A. Kanis, N. Norton, N.C. Harvey, T. Jacobson, H. Johansson, M. Lorentzon, E.V. McCloskey, C. Willers, F. Borgström, *Arch. Osteoporos* **16**, 82 (2021).

[7] GBD 2019 Fracture Collaborators, *Lancet Healthy Longev.* **2**, e580 (2021).

[8] G.S. Keene, M.J. Parker, G.A. Pryor, *Br. Med. J.* **307**, 1248 (1993).

[9] C.L. Leibson, A.N.A. Tosteson, S.E. Gabriel, J.E. Ransom, L.J. Melton, *J. Am. Geriatr. Soc.* **50**, 1644 (2002).

[10] P.M. Camacho, S.M. Petak, N. Binkley et al., *Endocr. Pract.* **26**, 1 (2020).

[11] B.R. Emmerson, M. Varacallo, D. Inman, *Hip Fracture Overview*, StatPearls Publishing, Treasure Island (FL) 2024.

[12] V. Hegde, J.B. Stambough, B.R. Levine, B.D. Springer, *Arthroplast. Today* **21**, 101137 (2023).

[13] L. Okafor, A.F. Chen, *Arthroplasty* **1**, 6 (2019).

[14] A.M. Negm, L.A. Beaupre, C.M. Goplen, C. Weeks, J.A. Jones, *Arthroplast. Today* **16**, 247 (2022).

[15] J.T. Evans, J.P. Evans, R.W. Walker, A.W. Blom, M.R. Whitehouse, A. Sayers, *Lancet* **393**, 647 (2019).

[16] G.R. Roytman, A.F. Ramji, B. Beitler, B. Yoo, M.P. Leslie, M. Baumgaertner, S.M. Tommasini, D.H. Wiznia, *Geriatr Orthop Surg Rehabil* **13**, 21514593221141376 (2022).

[17] M. Cristy, *Phys. Med. Biol.* **26**, 389 (1981).

[18] NIH 3D, 3D Models of the Female Thigh, Knee, and Leg Bones, 2024.

[19] M. Marco, E. Giner, J.R. Caeiro-Rey, M.H. Miguélez, R. Larraínzar-Garijo, *Comput. Methods Programs Biomed.* **173**, 67 (2019).

[20] A.A. Ali, L. Cristofolini, E. Schileo, H. Hu, F. Taddei, R.H. Kim, P.J. Rullkoetter, P.J. Laz, *J. Biomech.* **47**, 536 (2014).

[21] E. Schileo, L. Balistreri, L. Grassi, L. Cristofolini, F. Taddei, *J. Biomech.* **47**, 3531 (2014).